CHEMIJA
2025. Vol. 36. No. 4. P. 265–276

ISSN 0235-7216 eISSN 2424-4538
DOI: https://doi.org/10.6001/chemija.2025.36.4.6

Preparation and performance characterisation of organosilicon-modified cardanol-phenolic resins

Shusheng Gong[1],

Guomei Xu[1, 2],

Chen Han[1],

Chunfen Huang[3],

Hanjie Ying[2*]

Hongxue Xie[1, 4*]

[1] *Anhui Province Key Laboratory of Conservation and Utilization for Dabie Mountain Special Bio-Resources, School of Materials and Chemical Engineering, West Anhui University, Lu'an, Anhui 237012, China*

[2] *State Key Laboratory of Materials-Oriented Chemical Engineering, Nanjing Tech University, Nanjing, Jiangsu 210009, China*

[3] *School of Economics and Management, West Anhui University, Lu'an, Anhui 237012, China*

[4] *School of Engineering, Design and Built Environment, Western Sydney University, Locked Bag 1797, Penrith, NSW, 2751, Australia*

This study presents the synthesis and characterisation of KH550-modified cardanol-based phenolic hybrid resins. The hybrid resins were prepared via a two-step process: (1) synthesis of cardanol-based phenolic resin (CPR) through the condensation of cardanol and paraformaldehyde (1:1.3 molar ratio of phenolic hydroxyl groups to aldehyde groups), followed by (2) ultrasound-assisted grafting of γ-aminopropyltriethoxy silane (KH550) at varying mass ratios (5 and 15 wt%, denoted as CPR-K5 and CPR-K15, respectively). Hydrolysis of KH550 generated silanol (Si–OH) groups, which underwent covalent grafting and condensation reactions with the phenolic hydroxyl groups (–OH) and hydroxymethyl groups (–CH_2OH) of CPR to form Si–O–C crosslinked networks, as confirmed by Fourier transform infrared spectroscopy (FTIR) and X-ray photoelectron spectroscopy (XPS). Scanning electron microscopy (SEM) revealed the homogeneous dispersion of the organosilicon phase within the resin matrix. Thermogravimetric analysis (TGA) demonstrated a significant enhancement in thermal stability, with the char yield at 800°C increasing from 7.8% (neat CPR) to 22.1% (CPR-K15). Stress-strain tests verified the enhanced mechanical performance, with the Young's modulus of CPR-K5 reaching 104.7 MPa (representing a ~512% increase compared to neat CPR, 17.1 MPa) and that of CPR-K15 being 52.2 MPa (~205% increase vs neat CPR). This work provides a facile strategy for preparing sustainable hybrid resins with tailored thermomechanical properties, addressing the inherent brittleness and a low char yield of conventional cardanol-based phenolic resins. The resulting materials show potential for high-temperature structural applications and flame-retardant composites.

Keywords: cardanol, phenolic resin, γ-aminzopropyltriethoxy silane (KH550), phenolic aldehyde condensation, organosilicon-phenolic hybrid resins

INTRODUCTION

Cardanol, a natural phenolic monomer extracted from cashew nut shell liquid (CNSL), has gained a significant attention as a sustainable alternative to petroleum-derived phenol in polymer synthesis due to its renewable nature, cost-effectiveness and unique molecular architecture [1]. Characterised by a phenolic hydroxyl group (–OH) and a meta-substituted unsaturated C15 aliphatic chain, cardanol combines the reactivity of aromatic moieties, the flexibility of long-chain hydrocarbons, and

* Corresponding author. Email: yinghanjie@njtech.edu.cn

the functional tunability of phenolic compounds [2]. This structural versatility positions it as an ideal green feedstock for developing high-value polymers, particularly cardanol-based phenolic resins (CPRs), which hold promise to replace conventional petroleum-based phenolic resins (PFs) [3].

Phenolic resins, as classic thermosetting polymers, are extensively utilised in adhesives, flame-retardant coatings, corrosion-resistant materials and high-temperature structural components owing to their excellent thermal stability, chemical resistance and mechanical rigidity [4]. However, pristine CPRs inherit the intrinsic limitations of traditional PFs, including a high brittleness, a low char yield and an inferior thermomechanical performance [5]. These drawbacks restrict their applications in advanced fields such as high-temperature structural components and flame-retardant composites, where superior thermal stability and mechanical robustness are critical. To overcome these limitations, various modification strategies have been developed, encompassing chemical functionalisation, nanomaterial reinforcement [6] and hybridisation with organic/inorganic additives [7].

Among these approaches, hybridisation with organosilicon compounds has demonstrated efficacy in enhancing the comprehensive performance of phenolic resins. For instance, silane coupling agents like γ-aminopropyltriethoxy silane (KH550) can form covalent Si–O–C linkages with phenolic hydroxyl groups through hydrolysis-condensation reactions, thereby improving crosslinking density, thermal stability and mechanical properties [8]. As a commercially available silane coupling agent, KH550 is widely employed in polymer modification due to its reactive amino and ethoxy groups. Previous studies have shown that KH550 modification enhances char formation and interfacial compatibility in phenolic resins [9]. Nevertheless, the modification of CPRs with KH550 remains underexplored, and several critical research gaps persist [10]. Specifically, systematic investigations on the ultrasound-assisted grafting mechanism of KH550 onto CPRs are lacking. The impact of KH550 dosage on the structure–property relationships of CPR-based hybrid resins has not been fully elucidated. Moreover, the novelty of KH550-modified CPRs compared to existing organosilicon-modified phenolic resins requires clearer definition [11].

Herein, we propose a facile two-step strategy for preparing KH550-modified cardanol-based phenolic hybrid resins. First, CPR is synthesised via the condensation of cardanol and paraformaldehyde at a phenolic hydroxyl to aldehyde molar ratio of 1:1.3. Second, ultrasound-assisted grafting of KH550 is performed at mass ratios of 5 and 15%. The ultrasound-assisted process serves dual purposes: promoting a homogeneous dispersion of KH550 and facilitating hydrolysis-condensation reactions between silanol groups (generated from KH550 hydrolysis) and CPR's phenolic hydroxyl or hydroxymethyl groups to form a Si–O–C crosslinked network. This study pursues three primary objectives. First, it investigates the grafting mechanism and microstructural characteristics of hybrid resins using Fourier transform infrared spectroscopy (FTIR) and X-ray photoelectron spectroscopy (XPS). Second, it evaluates the effect of KH550 dosage on material properties, including thermal stability (via thermogravimetric analysis, TGA), mechanical performance (via stress-strain tests) and morphological features (via scanning electron microscopy, SEM). Third, it aims to enhance the thermal stability and mechanical properties of CPR. This work provides a straightforward approach to modify CPR with KH550, yielding resins with improved thermal and mechanical performances compared to pristine CPR, thus offering practical insights for modifying cardanol-based phenolic resins in relevant applications.

EXPERIMENTAL

Materials

Cardanol (molar mass M = 304.52 g·mol^{-1}) was provided by Shandong Haobo Biological Material Co., Ltd., Shandong, China. It is an industrial-grade product with a purity of ≥95% and presents as a pale yellow to brown viscous liquid at room temperature. Paraformaldehyde (industrial-grade, purity ≥96%) was purchased from Shanghai Chemical Reagents Company, Shanghai, China. Absolute ethanol (analytical-grade, purity ≥99.7%), sodium hydroxide (NaOH, analytical-grade, purity ≥98%) and silane coupling agent KH550 (γ-aminopropyltriethoxysilane, industrial-grade, purity ≥95%) were all obtained from Sinopharm Chemical Reagent Co., Ltd., China. Deionised water,

used throughout the experiment, was prepared in our laboratory using the ZKWL-2001 Ultrapure Water Purification System manufactured by Zhongke Ant Instrument Co., Ltd., China.

Synthesis of cardanol-based phenolic resin

Cardanol-based phenolic resin (CPR) was synthesised via a base-catalysed condensation reaction between cardanol and paraformaldehyde. Typically, 258 g of cardanol and 32 g of paraformaldehyde were precisely weighed [12], corresponding to a monomer molar ratio of 1:1.3 (phenolic hydroxyl groups to aldehyde groups, 1:1.3). Sodium hydroxide (2 g) was added as the condensation catalyst.

The reaction was carried out in a 500 mL three-neck round-bottom flask equipped with a reflux condenser, a mechanical stirrer and a temperature-controlled oil bath (RCT Basic, IKA). Cardanol was first charged into the flask and heated to 65°C under constant mechanical stirring at 300 rpm. Paraformaldehyde and NaOH were then added slowly to maintain controlled exothermic reaction conditions. Finally, a maroon sticky product was obtained. The resulting CPR (Fig. 1) was cooled to

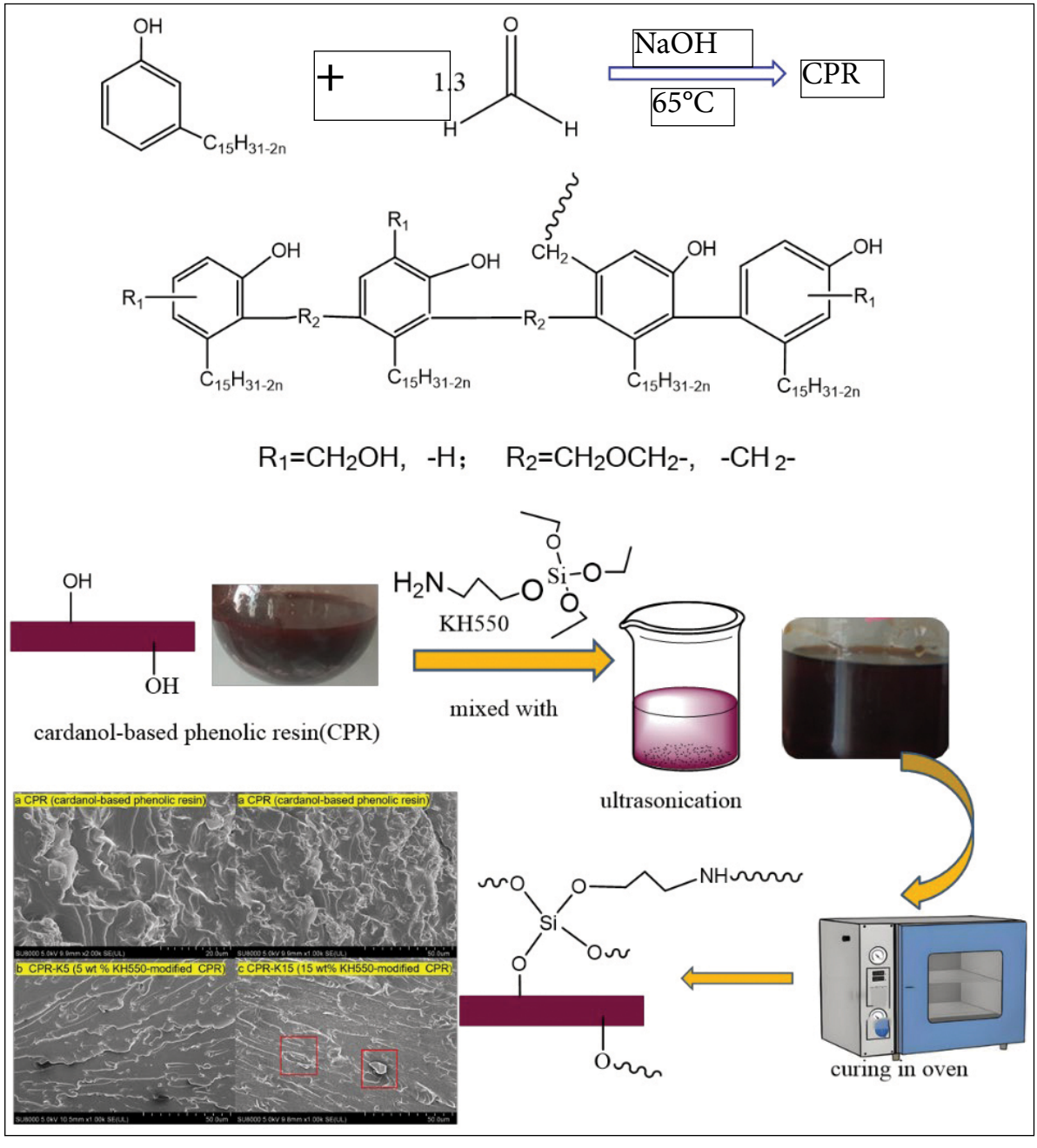

Fig. 1. Preparation route of the organosilicon-phenolic resins

room temperature and stored in a sealed container for subsequent modification.

Silane modification of CPR

CPR was functionalised with γ-aminopropyltriethoxysilane (KH550) to prepare silane-modified CPR samples, denoted as CPR-K5 (5 wt% KH550 relative to CPR) and CPR-K15 (15 wt% KH550 relative to CPR) for the consistent nomenclature throughout the manuscript.

The modification procedure was as follows. Firstly, 50 g of CPR was dissolved in 50 mL of anhydrous ethanol under magnetic stirring (RCT Basic, IKA) at 500 rpm for 10 min to form a homogeneous solution. Secondly, KH550 (5 or 15 wt% relative to CPR) was added dropwise to the resin solution under continuous magnetic stirring to ensure a uniform dispersion. The mixture was then transferred to a thermostated ultrasonic bath (KQ-250DE, Kunshan Ultrasonic Instrument Co., Ltd) and subjected to ultrasonication at 70 ± 1°C, 40 kHz and 150 W for 4 h. This ultrasonication process was intended to promote covalent grafting, specifically between the silanol (Si–OH) groups generated by KH550 hydrolysis and the phenolic hydroxyl groups (–OH) as well as hydroxymethyl groups (–CH_2OH) of CPR, which was subsequently confirmed by FTIR analysis.

Subsequently, residual ethanol was evaporated under reduced pressure using a rotary evaporator (RV3V, IKA) at 60 ± 1°C and 0.1 Mpa, yielding the silane-modified phenolic resin composites (CPR-K5 and CPR-K15).

Thermal curing of composites

The modified composites were placed into a stainless-steel mold and cured in an air-circulating oven using a stepwise temperature program. The curing protocol consisted of an initial isothermal hold at 80°C for 2 h, followed by incremental 20°C increases (100, 120, 140, 160 and 180°C), each maintained for 2 h. Finally, the temperature was raised to 200°C for additional 2 h to ensure complete crosslinking. The resulting specimens were demolded after cooling to room temperature.

Measurements

Fourier-transform infrared spectroscopy (FTIR) analysis was conducted on a Thermo Fisher iS50 spectrometer with a resolution of 4 cm^{-1} and 32 scans, scanning over a wavenumber range of 500–4000 cm^{-1} using KBr pellets (sample-to-KBr mass ratio of 1:100, pressed under 10 MPa for 30 s). Morphological characterisation was performed using field-emission scanning electron microscopy (FE-SEM, FEI Sirion 200) at an accelerating voltage of 3 kV. Thermal stability was evaluated by thermogravimetric analysis (TGA, TA Instruments Q5000) under high-purity nitrogen atmosphere (purity ≥99.999%) with a gas flow rate of 100 mL/min. Approximately 5–10 mg of each sample was loaded into alumina crucibles, and the measurements were conducted from ambient temperature (25°C) to 800°C at a constant heating rate of 10°C/min. The surface chemical composition analysis of CPR before and after modification was carried out via X-ray photoelectron spectroscopy (XPS) using a Thermo-VG Scientific ESCALAB 250 system. Measurements were performed with a monochromatic Al Kα X-ray source ($h\nu$ = 1486.6 eV) operating at 15 kV and 10 mA. Survey spectra were collected over a binding energy range of 0–1200 eV with a step size of 1 eV and a pass energy of 100 eV. Peak fitting was performed using the XPS Peak 4.1 software with the Shirley-type background correction. Stress ramp test (Instron 0850-00252, RT): The mechanical properties of the modified resins were systematically evaluated via stress ramp tests. Specimens with dimensions of 7.41 × 8.40 × 0.97 mm^3 were tested at a loading rate of 2 mm/min.

RESULTS AND DISCUSSION

FTIR spectra of cardanol, CPR and KH550-modified CPR

Fourier-transform infrared (FTIR) spectroscopy was employed to characterise the structural changes of cardanol, pristine cardanol-based phenolic resin (CPR) and KH550-modified CPR (CPR-K5 with 5 wt% KH550 and CPR-K15 with 15 wt% KH550) during synthesis and modification. The comparative spectra of cardanol and CPR (Fig. 2) include the full wavenumber range from 500 to 4000 cm^{-1}, along with the magnified views of crucial regions between 600 and 2000 cm^{-1}. Cardanol (Fig. 2) presents distinct absorption peaks. The peaks at 2926 and 2859 cm^{-1} are attributed to aliphatic C–H stretching vibrations. The peak at 3011 cm^{-1} corresponds to the C–H stretching vibrations of C=C double bonds [13]. The broad peak at 3441 cm^{-1} is assigned to

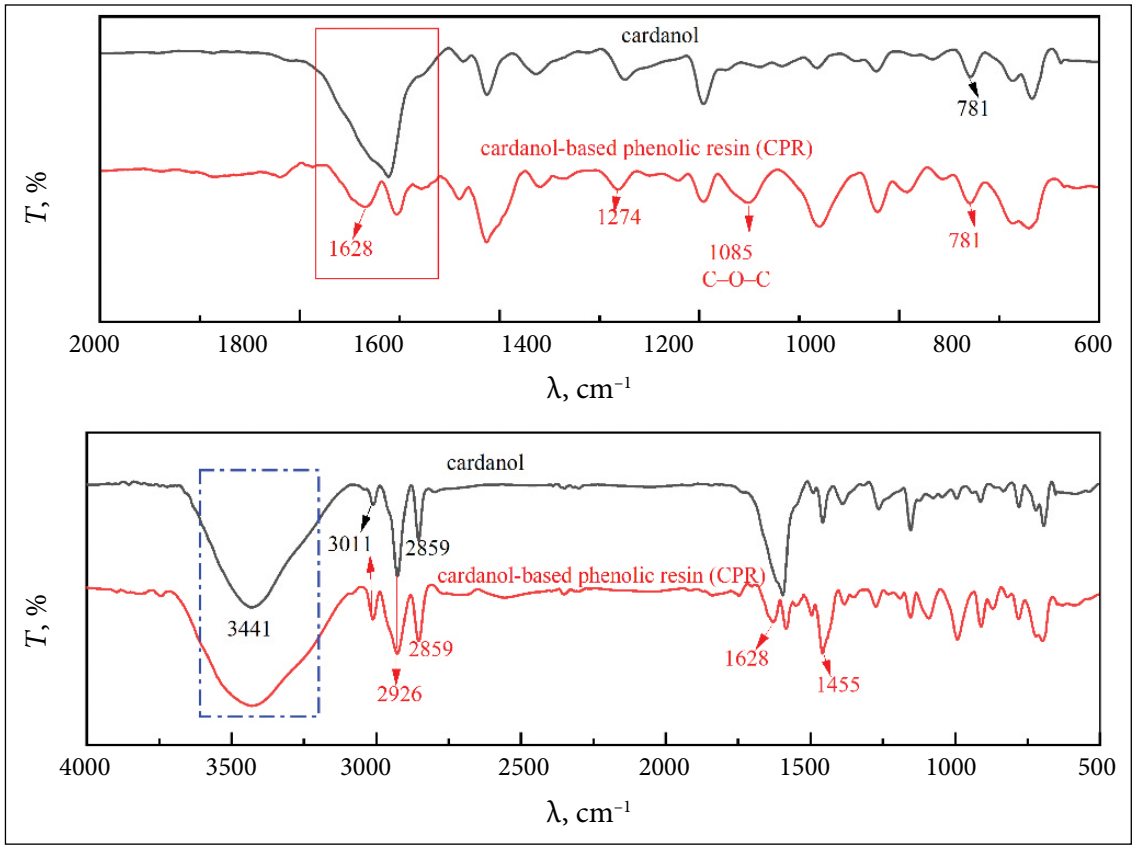

Fig. 2. FTIR spectra of cardanol and CPR

the O–H stretching vibrations of phenolic hydroxyl groups [14]. Additionally, the peak at 781 cm^{-1} represents the out-of-plane bending vibrations of C–H in ortho/meta-disubstituted benzene rings. These peaks collectively confirm that cardanol contains reactive phenolic hydroxyl groups and unsaturated side chains, which serve as essential active sites for subsequent polycondensation reactions. CPR (Fig. 2) exhibits unique spectral features. The broadened O–H stretching vibration peak at 3441 cm^{-1} is due to intermolecular hydrogen bonding. The peak near 1000 cm^{-1} is associated with hydroxymethyl groups ($–CH_2OH$) [15]. The peak at 1085 cm^{-1} corresponds to C–O–C, representing anisole linkages. The peak at 1274 cm^{-1} is attributed to aromatic C–O stretching vibrations [16]. The peak at 1455 cm^{-1} corresponds to methylene groups ($–CH_2–$) [17], and the peak at 1628 cm^{-1} is due to aromatic C=C stretching vibrations. The retention of the 781 cm^{-1} peak confirms that the benzene rings are in ortho/meta-disubstituted configurations and that the integrity of the aromatic ring backbone remains intact. These characteristics indicate that the product is a polymer linked by $–CH_2O–/–CH_2–$, which is consistent with the structure of phenolic resin oligomers. CPR is soluble in ethanol and appears burgundy, which further confirms the successful synthesis of a low-molecular-weight phenolic resin.

KH550-modified CPR (Fig. 3) retains the main structural features of pristine CPR while exhibiting new absorption peaks corresponding to the introduced organosilicon and amino functional groups. Key absorption peaks of the modified resins include: 3441 cm^{-1} (O–H stretching vibrations, due to intermolecular hydrogen bonding); 2926/2859 cm^{-1} (aliphatic C–H stretching vibrations); 1541 cm^{-1} (N–H bending vibrations, indicating interactions between the amino group of KH550 and CPR) [18]; 1271/1130 cm^{-1} (asymmetric stretching vibrations of Si–O–Si, confirming the formation of polysiloxane networks) [19].

The intensity of the characteristic peak for hydroxymethyl groups ($–CH_2OH$) near 1000 cm^{-1} is significantly reduced in CPR-K5 and CPR-K15 compared to pristine CPR. This intensity diminution confirms the participation of hydroxyl groups (phenolic –OH and aliphatic $–CH_2OH$) in CPR in condensation reactions. The underlying mechanism

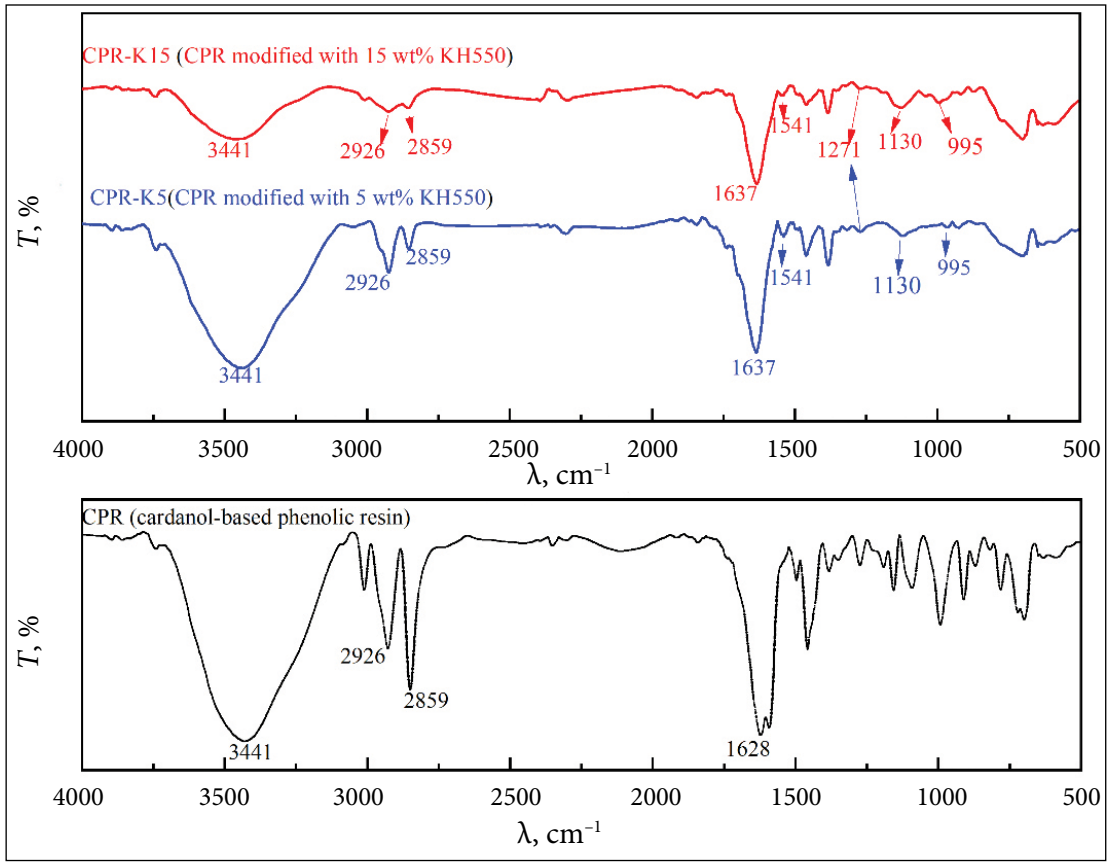

Fig. 3. FTIR spectra of the organosilicon-phenolic resins

is as follows. KH550 undergoes hydrolysis to generate silanol groups (Si–OH), which react with the hydroxyl groups in CPR to form Si–O–C covalent bonds. This reaction consumes many free and hydrogen-bonded hydroxyl groups in the system, thereby reducing the absorption intensity of the corresponding characteristic peak at 1000 cm^{-1}. Regarding the characteristic peak for Si–O–Ph (siloxyphenyl groups) at 995 cm^{-1}, it appears as a broad peak with a weak intensity in both CPR-K5 and CPR-K15. This phenomenon may be attributed to two factors: (1) the low grafting degree of KH550, resulting in a low content of Si–O–Ph linkages; (2) KH550 preferentially reacts with aliphatic $–CH_2OH$ rather than aromatic phenolic –OH, leading to the formation of more Si–O–C linkages with aliphatic chains instead of Si–O–Ph linkages. This conclusion requires further verification by X-ray photoelectron spectroscopy (XPS). In summary, the retention of phenolic resin characteristic peaks (1637 and 1271 cm^{-1}) confirms the integrity of the CPR matrix after modification, while the emergence of organosilicon (1271/1130 cm^{-1}) and amino (1541 cm^{-1}) characteristic peaks verifies the successful introduction of KH550.

XPS analysis

To verify the chemical interaction between KH550 and the phenolic resin after ultrasonic treatment, the purified and dried modified samples were subjected to X-ray photoelectron spectroscopy (XPS) characterisation. As illustrated in the survey spectrum of Fig. 4a, in addition to the intrinsic C (~285 eV) and O (~532 eV) signals, the characteristic signal of Si (at ~100 eV, marked with an arrow) is clearly identified. No obvious N signal (around 400 eV) was detected, which may be related to the detection limit of XPS and the grafting state of KH550. The elemental composition of the modified resin surface is determined as Si (1.05%), C (88.27%) and O (10.68%). The presence of the Si signal provides the direct evidence for the successful incorporation of KH550-derived moieties into the resin matrix, which is consistent with the FTIR results.

To elucidate the binding states of C, O and Si in the modified resin, high-resolution spectra of C

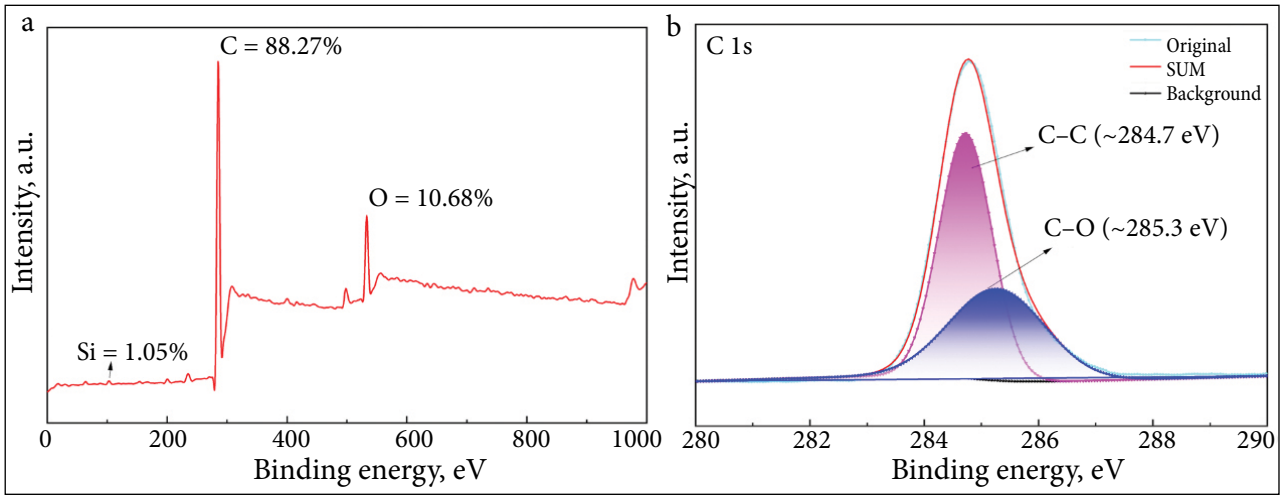

Fig. 4. Surface elements (a) and C 1s XPS spectra (b) of the organosilicon-phenolic resins

1s, O 1s and Si 2p (Fig. 4b, Fig. 5a, b, respectively) were deconvoluted using the Shirley-type background correction. The C 1s spectrum (Fig. 4b) exhibits two well-resolved peaks at 284.7 and 285.3 eV, which are assigned to C–C/C–H bonds (aliphatic and aromatic carbon skeletons) and C–O bonds (phenolic hydroxyl and ether linkages), respectively [20]. These peaks are characteristic of the phenolic resin backbone, confirming the integrity of the CPR matrix after modification.

The O 1s spectrum (Fig. 5a) can be deconvoluted into three distinct contributions: 531.7 eV (hydroxyl groups, –OH), 532.7 eV (Si–O bonds, from siloxane networks or Si–O–C linkages) and 533.6 eV (C–O moieties, from phenolic ether or aliphatic ether groups). The emergence of the Si–O peak at 532.7 eV directly evidences the formation of siloxane networks and covalent linkages between KH550 and CPR, which is consistent with the FTIR results of Si–O–Si characteristic peaks. Notably, no N signal was detected in either the survey spectrum or the high-resolution spectra. This phenomenon can be reasonably explained by the following factors. Firstly, the grafting degree of KH550 is relatively low, resulting in the N content on the resin surface being below the detection limit of XPS. Secondly, XPS is a surface-sensitive technique (detection depth: 2–10 nm), and KH550-derived moieties may be preferentially embedded in the inner layer of the resin matrix rather than enriched on the surface, leading to undetectable N signals. Thirdly, the amino groups of KH550 may undergo further reactions (e.g. crosslinking with residual hydroxymethyl groups) to form structures that are difficult

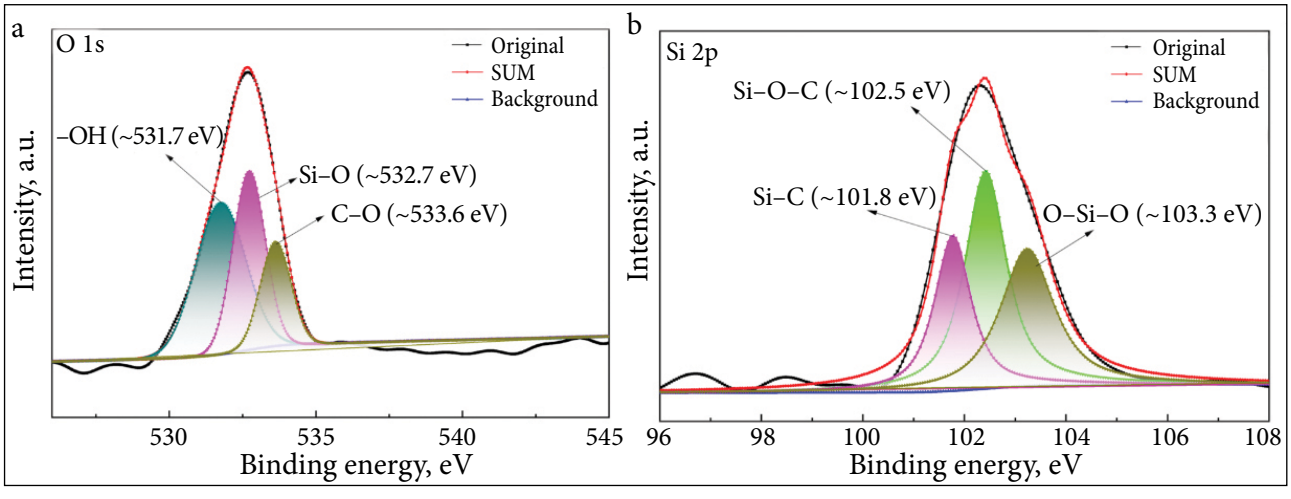

Fig. 5. O 1s (a) and Si 2p (b) XPS spectra of the organosilicon-phenolic resins

to distinguish, but this does not affect the main grafting reaction between Si-containing groups and CPR. Although no N signal was detected, the presence of Si signal and the FTIR characteristic peak of N–H (1541 cm^{-1}) collectively confirm the introduction of KH550, reflecting the difference in the surface and bulk information between XPS and FTIR.

The Si 2p spectrum (Fig. 5b) manifests three chemically distinct states: Si–C (101.8 eV), siloxane bridges (O–Si–O, 103.3 eV) and Si–O–C (102.5 eV) [21]. The presence of the Si–O–C peak further confirms the occurrence of intermolecular condensation reactions between silanol groups (Si–OH) derived from KH550 hydrolysis and hydroxyl groups (–OH/–CH_2OH) of CPR, leading to the formation of covalent linkages between the organosilicon component and the phenolic matrix. These intermolecular condensation reactions contribute to the formation of Si–O–C covalent linkages and the crosslinked network of the hybrid resin, which is further supported by the C 1s, O 1s and Si 2p XPS results.

In conclusion, the XPS analysis (survey spectrum and high-resolution Si 2p spectrum) confirms the successful incorporation of KH550 into the CPR matrix via covalent linkages (Si–O–C) and the formation of a polysiloxane crosslinked network. The absence of N signal is attributed to the low surface N content (below the XPS detection limit) or the preferential embedding of KH550-derived moieties in the resin inner layer, which is not contradictory to the FTIR result of the N–H characteristic peak.

Thermal stability evaluation via TGA

Figure 6 compares the thermogravimetric (TGA) curves of pristine cardanol-based phenolic resin (CPR) and its KH550-modified counterparts (CPR-K5, 5 wt%; CPR-K15, 15 wt%).

Three distinct thermal degradation stages are observable for all samples under nitrogen (N_2) atmosphere (flow rate: 100 mL/min; heating rate: 10°C/min; temperature range: 25–800°C). The unmodified CPR starts to lose mass at 265°C, which is attributed to the pyrolytic cleavage of phenolic hydroxyl groups and aliphatic side chains. In contrast, the KH550-modified resins (CPR-K5 and CPR-K15) exhibit a delayed decomposition onset (300°C) compared to pristine CPR, confirming the enhanced thermal stability induced by organosilicon modification. For key thermal stability metrics, CPR shows 5 and 10% mass loss at 298 and 328°C, respectively. Notably, CPR-K5 demonstrates a superior early-stage thermal stability, with 5 and 10% mass loss at

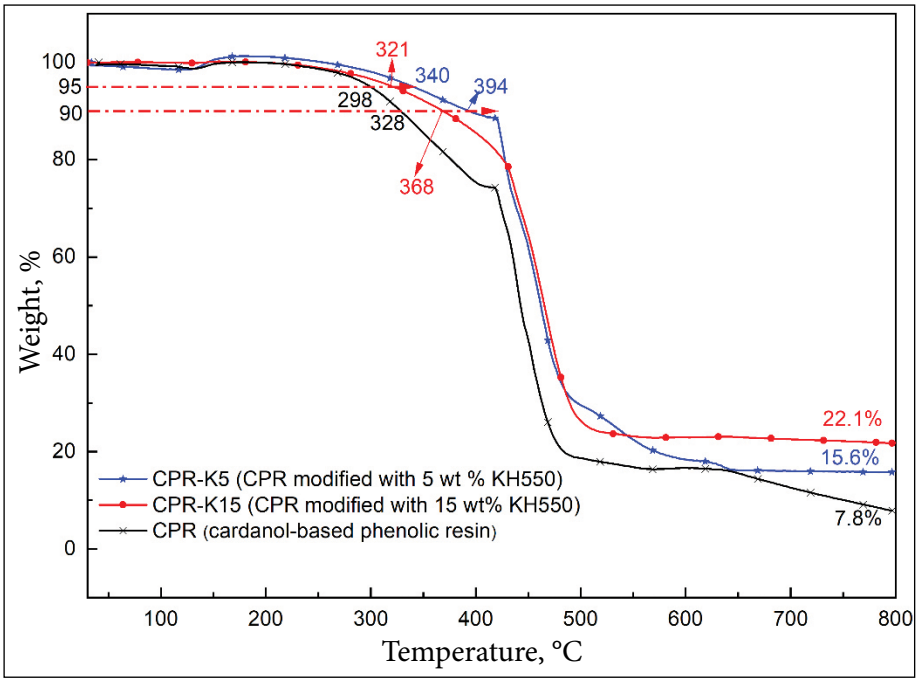

Fig. 6. TGA curves of the prepared product

340 and 394°C, respectively. Meanwhile, CPR-K15 shows an intermediate behaviour relative to CPR-K5, with 5% mass loss at 321°C and 10% mass loss at 368°C.

At 800°C, the residual char yields follow a different order compared to the early-stage mass loss thresholds: CPR-K15 (22.15 wt%) > CPR-K5 (15.60 wt%) > CPR (7.80 wt%). This non-monotonic trend (CPR-K5 exhibiting a superior early-stage stability while CPR-K15 showing a superior char yield) can be reasonably explained by the following mechanisms: (1) At a low KH550 loading (5 wt%, CPR-K5), KH550 is uniformly dispersed in the CPR matrix, forming dense Si–O–C crosslinked points that efficiently suppress the initial cleavage of hydroxyl and aliphatic groups, thereby improving early-stage thermal stability. (2) At a higher KH550 loading (15 wt%, CPR-K15), a slight local aggregation of KH550 may occur, leading to a mild compromise in early-stage degradation resistance. However, the higher content of silicon-containing groups promotes the formation of a continuous, thermally stable silicate-rich char layer during high-temperature degradation (800°C), which inhibits further volatilisation of degradation products and enhances char retention efficiency. This observation highlights the dual effects of KH550 loading on thermal stability and provides guidance for optimising the KH550 dosage based on application requirements (early-stage heat resistance versus high-temperature char formation).

The enhanced thermal resistance of the modified resins originates from siloxane crosslinking via condensation reactions between KH550-derived silanol (Si–OH) groups and CPR's hydroxyl (–OH)/hydroxymethyl (–CH_2OH) groups, forming Si–O–C crosslinked networks [22]. This crosslinking effect is corroborated by Fourier-transform infrared spectroscopy (FTIR) (the emergence of Si–O–Si peaks at 1271/1130 cm^{-1} and a reduced intensity of the –CH_2OH peak at 1000 cm^{-1}) and X-ray photoelectron spectroscopy (XPS) (the detection of Si–O–C bonds at 102.5 eV in the Si 2p spectra), which confirm the formation of covalent linkages and polysiloxane networks. The Si–O–Si bonds in the crosslinked network (bond energy ≈ 452 kJ/mol) suppress the heterogeneous cleavage of the phenolic backbone at elevated temperatures [23], retard the release of volatile degradation products (e.g. phenols, H_2O, CO_x) via steric hindrance effects and promote condensed-phase carbonisation pathways. These effects collectively contribute to the elevated thermal stability and char yields observed in the modified samples, with the extent depending on the KH550 loading and dispersion state.

Mechanical properties evaluation via stress ramp tests

The mechanical properties of multi-stage thermally cured KH550-modified phenolic resins were systematically evaluated via stress ramp tests. Specimens with dimensions of $7.41 \times 8.40 \times 0.97$ mm^3 were tested on an Instron 0850-00252 at room temperature with a loading rate of 2 mm/min. The stress-strain profiles derived from the stress ramp tests are presented in Fig. 7.

To provide the quantitative support for the claim of enhanced mechanical strength, the Young's modulus was calculated for each sample. The Young's modulus (E) was determined from the slope of the initial linear portion of the stress–strain curve, following the formula

$$E = \frac{\sigma}{\varepsilon},$$

where σ is the stress and ε is the strain. The results show that the Young's modulus of pristine CPR is 17.1 MPa, while that of CPR-K5 (5 wt% KH550) reaches 104.7 MPa (an approximately 512% increase relative to pristine CPR), and CPR-K15 (15 wt% KH550) is 52.2 MPa (an approximately 205% increase versus pristine CPR). The mechanical enhancement trend is clearly validated by the comparison among CPR, CPR-K5 and CPR-K15: CPR-K5 (104.7 MPa) > CPR-K15 (52.2 MPa) > CPR (17.1 MPa). For CPR-K5, the uniform dispersion of KH550 promotes dense intermolecular condensation reactions between silanol (Si–OH) groups (derived from KH550 hydrolysis) and hydroxyl groups (–OH/–CH_2OH) in CPR, forming a homogeneous Si–O–C crosslinked network [24]. This network restricts molecular chain mobility via topological constraints, enables an efficient stress transfer across Si–O–C interfaces and mitigates crack propagation through energy-dissipative siloxane domains [38]. For CPR-K15, despite achieving

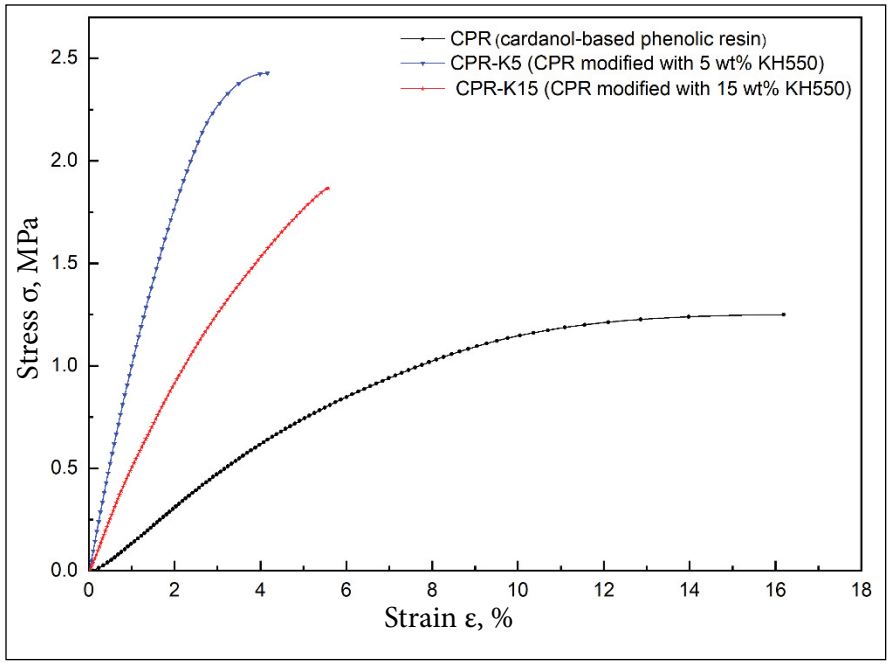

Fig. 7. Stress–strain curves of the prepared products

an approximately 205% increase in Young's modulus compared to CPR, its stiffness is lower than that of CPR-K5. This is attributed to a slight local aggregation of KH550 (inferred from TGA), which results in an uneven crosslink density and a localized stress concentration during loading, thereby undermining the mechanical enhancement efficiency compared to the uniformly dispersed CPR-K5. With the Young's modulus data of both CPR-K5 (104.7 MPa) and CPR-K15 (52.2 MPa) obtained from stress ramp tests, the non-proportional mechanical enhancement versus KH550 content is confirmed. The stiffness enhancement efficiency of CPR-K5 is significantly higher than that of CPR-K15. This non-monotonic trend stems from competing effects: (1) At low KH550 loading (5 wt%, CPR-K5), a uniform dispersion dominates, promoting the formation of a homogeneous Si–O–C crosslinked network that efficiently enhances stiffness [25]; (2) At higher KH550 loading (15 wt%, CPR-K15), a localised aggregation becomes prominent, leading to an uneven crosslink density and aggregation-induced defects, which offset part of the stiffness enhancement from the increased crosslink content [26]. The intrinsic origin of mechanical reinforcement lies in covalent conjugation between siloxane moieties (≡Si–O–) and reactive hydroxyl/hydroxymethyl groups in the phenolic network, which is corroborated by the reduced intensity of the $-CH_2OH$ peak (1000 cm^{-1}) in the FTIR spectra and the detection of Si–O–C bonds in XPS spectra.

Morphological evolution via SEM

Figure 8 presents the cross-sectional morphologies of phenolic resins with varying KH550 mass fractions. The SEM micrographs reveal a progressive densification of the resin matrix with increasing KH550 content. Specifically, Fig. 8a shows the cross-sectional morphology of neat phenolic resin (CPR). It exhibits obvious wrinkled features [27]. In contrast, Fig. 8b (CPR-K5, 5 wt% KH550) and Fig. 8c (CPR-K15, 15 wt% KH550) demonstrate that as the mass fraction of KH550 increases, the surface of the phenolic resin becomes increasingly dense, and the wrinkled features gradually diminish or even disappear.

As shown in Fig. 8c (CPR-K15), there is a solid accumulation on the surface, while the surface in Fig. 8b (CPR-K5) appears relatively uniform. This morphological transition (from a wrinkled appearance to a uniform one and then to solid accumulation) aligns with the inferences drawn from previous TG and XPS results [28]. XPS analysis confirms that the content of Si–O–C covalent bonds (formed through the co-condensation of KH550 and phenolic resin) increases with the dosage of KH550, and

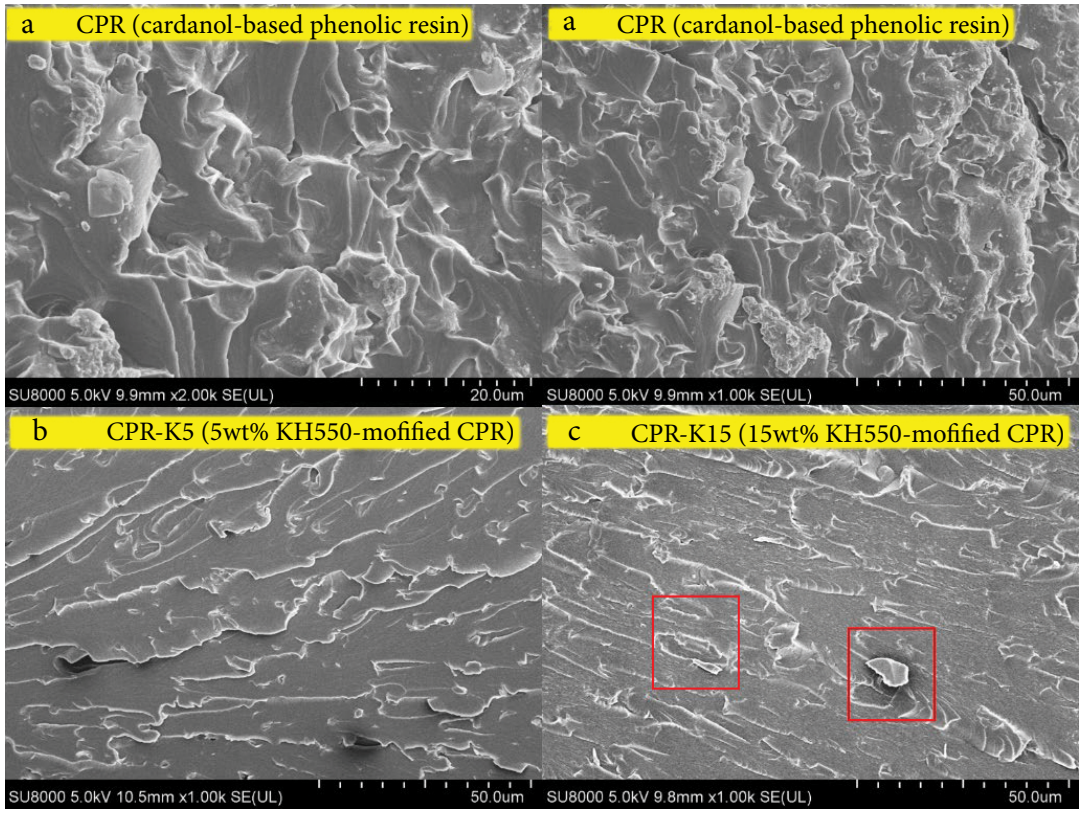

Fig. 8. SEM images of the prepared products

the TG results indicate an improvement in thermal stability resulting from the progressive densification of the matrix. Meanwhile, this morphological evolution also corroborates the tensile test results. The relatively uniform surface of CPR-K5 (Fig. 8b) facilitates better stress distribution, leading to higher tensile strength and elongation, while the solid accumulation on CPR-K15 (Fig. 8c) may induce a local stress concentration, which aligns with the slight fluctuation in the tensile performance of the sample with 15 wt% KH550; in comparison, the wrinkled structure of neat CPR (Fig. 8a) hinders stress transfer, resulting in lower tensile strength compared to KH550-modified samples.

CONCLUSIONS

This study investigated the structural, thermal and mechanical properties of KH550-modified cardanol-phenolic resin (CPR). The FTIR and XPS confirmed covalent Si–O–C bond formation, creating a silicone-cardanol hybrid composite. The TG analysis showed that modified CPRs exhibit enhanced thermal stability (e.g. CPR-K15: 22.1% char yield at 800°C vs neat CPR: 7.8%). The mechanical testing revealed that CPR-K5 achieved 104.7 MPa Young's modulus (512% higher than neat CPR), while CPR-K15 showed 52.2 MPa (205% higher). SEM correlated those improvements with morphological changes. KH550 modification at 5 wt% optimises CPR performance, offering quantitative guidance for high-temperature/flame-retardant applications.

ACKNOWLEDGEMENTS

This work was supported by the State Key Laboratory of Materials-Oriented Chemical Engineering (No. SKL-MCE-22B05); Key Project of Natural Science Research in Universities of Anhui Province, No. KJ2021A0941; the Undergraduate Innovation Project (202410376083, wxxy2025052); Natural Science Foundation of West Anhui University (WXZR202435, WXZR202401), College Students Innovative Entrepreneurial Training Plan Program (WXXY2024024, S202510376166), Process Development for Preparation of Electrospun Collagen Nanofibers (0045024037), Technical Services for Preparation of Electrospun Carbon-based Nanofiber Materials (0045022056), Testing and Characterization of Magnetic Nanofibers (0045025025).

This work was also supported by the Anhui Huahui Plastic Industry Technology Co., Ltd.

Received 18 October 2025
Accepted 8 December 2025

References

1. M. Patel, P. Rathva, M. Raj, L. Raj, *J. Polym. Environ*., **33**, 3987 (2025) [https://10.1007/s10924-025-03576-7].
2. S. K. Kyei, W. I. Eke, G. Darko, O. Akaranta, *J. Coat. Technol. Res.*, **19**, 775 (2022) [https://10.1007/s11998-021-00604-8].
3. B. Lochab, S. Shukla, I. K. Varma, *RSC Adv*., **4**, 21712 (2014) [https://10.1039/c4ra00181h].
4. W. Shen, D. Zhenzhen, L. Jiechao, F. Jianglei, L. Yachao, L. Jianxiu, *J. Electron. Mater.*, **52**, 8086 (2023) [https://10.1007/s11664-023-10728-9].
5. Q. Wei, W.-H. Wang, *Int. J. Adhes. Adhes.*, **84**, 166 (2018) [https://10.1016/j.ijadhadh.2018.03.006].
6. S. Wang, S. Zhou, J. Huang, G. Zhao, Y. Liu, *J. Mater. Sci.*, **54**, 8247 (2019) [https://10.1007/s10853-019-03512-w].
7. M. R. Esfahani, S. A. Aktij, Z. Dabaghian, et al., *Sep. Purif. Technol.*, **213**, 465 (2019) [https://10.1016/j.seppur.2018.12.050].
8. L. Zhou, T. Yin, Y. Fu, *Ceram. Int.*, **46**, 23236 (2020) [https://10.1016/j.ceramint.2020.06.108].
9. W. Wu, J. Wang, *Silicon*, **10**, 1903 (2018) [https://10.1007/s12633-017-9700-4].
10. T. Wang, S. Chen, H. Feng, L. Cao, Z. Zhao, W. Li, *Surf. Sci. Technol.*, 1 (2023) [https://10.1007/s44251-023-00028-z].
11. S. Eral, B. Oktay, C. Dizman, N. Kayaman Apohan, *Polym. Bull.*, **81**, 6873 (2023) [https://10.1007/s00289-023-05037-4].
12. G. Xu, T. Shi, Y. Xiang, W. Yuan, Q. Wang, *RSC Adv.*, **5**, 77429 (2015) [https://10.1039/c5ra10083f].
13. J. Yuan, Z. Zhang, M. Yang, F. Guo, X. Men, W. Liu, *Tribol. Int.*, **107**, 10 (2017) [https://10.1016/j.triboint.2016.11.013].
14. H. Ardhyananta, T. Kawauchi, H. Ismail, T. Takeichi, *Polymer*, **50**, 5959 (2009) [https://10.1016/j.polymer.2009.10.001].
15. Y. Jing, Y. Lu, K. Zhang, *Polym. Bull.*, **82**, 6613 (2025) [https://10.1007/s00289-025-05798-0].
16. Y. Zhang, X. Yang, J. Bao, et al., *Front. Chem. Sci. Eng.*, **17**, 504 (2023) [https://10.1007/s11705-022-2260-1].
17. D. G. Oke, E. O. Faboro, A. K. Oyebamiji, L. Labunmi, *Chem. Afr.*, **7**, 1889 (2024) [https://10.1007/s42250-023-00856-4].
18. Z. Zhu, Y. Liu, G. Xian, et al., *Macromol. Res.*, **31**, 771 (2023) [https://10.1007/s13233-023-00160-7].
19. S. Jeyachandran, T. Marimuthu, *Silicon*, **16**, 1823 (2023) [https://10.1007/s12633-023-02809-5].
20. H. Lee, S. Kim, J. Hwang, S. H. Kim, *Macromol. Res.*, **33**, 1421 (2025) [https://10.1007/s13233-025-00427-1].
21. M. Li, Z. Zhu, R. Jiao, et al., *J. Colloid Interface Sci.*, **654**, 719 (2024) [https://10.1016/j.jcis.2023.10.073].
22. Z. Fan, W. Xu, Y. Tian, X. Yang, R. Ni, *J. Polym. Environ.*, **32**, 3208 (2024) [https://10.1007/s10924-023-03158-5].
23. Z. Lu, Z. Liu, Z. Hu, L. Zhao, Z. Jia, Z. Rui, *Chem. Eng. J.*, 523 (2025) [https://10.1016/j.cej.2025.168866].
24. J. Thamilarasan, R. Ganesamoorthy, *Biomass Conv. Biorefin.*, **15**, 12189 (2024) [https://10.1007/s13399-024-06102-2].
25. X. Luo, F. Gao, F. Chen, et al., *RSC Adv.*, **10**, 15881 (2020) [https://10.1039/d0ra01279c].
26. Y. Li, W. Liu, J. Zhang, L. Song, K. Li, *Int. J. Metalcast*., **19**, 3773 (2025) [https://10.1007/s40962-025-01584-w].
27. S. Jeyachandran, P. Pichaimani, S. Gopalsamy, T. Marimuthu, *Silicon*, **17**, 2509 (2025) [https://10.1007/s12633-025-03347-y].
28. Y. Tong, L. Li, J. Liu, K. Zhang, Y. Jiang, *Mater. Res. Express*, 6 (2019) [https://10.1088/2053-1591/ab30d2].

Shusheng Gong, Guomei Xu, Chen Han, Chunfen Huang, Hanjie Ying, Hongxue Xie

ORGANINIO SILICIO MODIFIKUOTŲ KARDANOLIO-FENOLIO DERVŲ PARUOŠIMAS IR EKSPLOATACINIŲ SAVYBIŲ APIBŪDINIMAS